34th Annual International Conference of the IEEE EMBS
San Diego, California USA, 28 August - 1 September, 2012

Simultaneous Dielectric Monitoring of Microfluidic Channels at Microwaves Utilizing a Metamaterial Transmission Line Structure

M. Schüßler, M. Puentes, D. Dubuc, K. Grenier, and R. Jakoby

Abstract— **The paper presents a technique that allows the simultaneous monitoring of the dielectric properties of liquids in microfluidic channels at microwave frequencies. It is capable of being integrated within the lab-on-a-chip concept and uses a composite right/left-handed transmission line resonator which is detuned by the dielectric loading of the liquids in the channels. By monitoring the change in the resonance spectrum of the resonator the loading profile can be derived with the multi-resonant perturbation method. From the value of the dielectric constant inference on the substances like cells or chemicals in the channels can be drawn. The paper presents concept, design, fabrication and characterization of prototype sensors. The sensors have been designed to operate between 20 and 30 GHz and were tested with water and water ethanol mixtures.**

I. Introduction

Biosensors will enable the automatized and fast measurement of complex biochemical parameters that are usually destined for cumbersome laboratory work. The "lab-on-a-chip" approach allows the integration of different biosensors to elaborate systems, which are realized with microtechnology. Within the framework of this technology microfluidic structures for electromagnetic sensors operating in the vast frequency range from low frequencies, to Terahertz and optics have proven to bear a highly innovative potential for biosensors [1,2]. Among them microwave sensors have demonstrated the possibility to operate noninvasive, contactless, without the necessity to use markers or other modifications for a quick and precise real time monitoring of very small volumes [3,4].

The sensor concept presented in this paper works at microwave frequencies. In contrast to many sensors that allow the broadband characterization of a liquid in one channel [5,6], this sensor aims for the simultaneous monitoring of the dielectric constant in a small frequency band in several channels. Typical field of application is the parallelization in surveillance of known substances e.g. like living cells [6], or chemicals in micro reactors. The sensor is capable of real time monitoring at microwaves via one RF terminal without the necessity of using switches. Although demonstrated for the microwave regime the sensor principle is extendable to mm-wave and lower THz bands.

M. Schüßler, M. Puentes and R. Jakoby are with the Technische Universität Darmstadt, Institute of Microwave Engineering and Photonics, Merckstrasse 25, D-64283 Darmstadt, Germany, corresponding author is M. Schüßler, phone: +49-6151-163752, fax: +49-6151-164322, e-mail: schuessler@imp.tu-darmstadt.de.

D. Dubuc and K. Grenier are with LAAS CNRS, Fluidic High Frequency Micro and Nanosystems Group, LAAS-CNRS 7, avenue du Colonel Roche 31077 Toulouse Cedex 4, France.

II. Concept

The sensor's equivalent circuit is depicted in Fig. 1. It consists of a periodical arrangement of identical circuits that are called unit cells. The overall circuit is called composite right/left-handed transmission line (CRLH TL) and consist of n_c unit cells. The electromagnetic properties of such circuits have been extensively studied so that there is a well established theory available to describe their properties. It can be shown that the bandwidth requirement of a CRLH TL based sensor for this application is significantly small than with a conventional TL [7].

In each unit cell one capacitor labeled $C_{L,n}$ is implemented in a way that it is electromagnetically coupled with an adjacent microfluidic channel. Hence, the dielectric constant[1] of the liquid in the channel ($\varepsilon+\Delta\varepsilon_n$) influences the capacitance value $C_{L,n}$. The sensitive part of $C_{L,n}$ is labeled $C_{M,n}$ and the fixed part C_0. The ratio between C_M and C_0 is controlled by the geometrical placing of the microfluidic channel. With the help of the multi-resonant perturbation method (MRPM) [7] the dielectric loading of the microfluidic channels from Fig. 1 $[\Delta\varepsilon_1\ \Delta\varepsilon_2\ \ldots\ \Delta\varepsilon_n]^T$ can be derived based on a measurement of the CRLH TL properties.

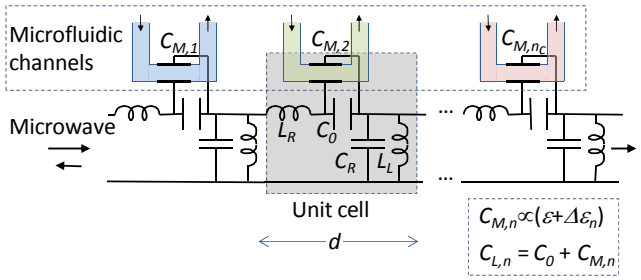

Figure 1. Schematic of the presented sensor. It consist of a CRLH TL, where a part of the left-handed capacitors $C_{L,n}$ are electromagnetically coupled to microfluidic channels. Hence the dielectric properties of the liquids in the channels change the electric properties of the transmission line.

[1] It should be noted that throughout the paper we will refer to the relative dielectric constant as ε and $\Delta\varepsilon$ and not ε_r and $\Delta\varepsilon_r$. The index "r" is used in the paper to denote "resonance".

The general formulation of the resonant perturbation method relates the frequency shift in a resonance frequency $\Delta\omega_r$ of a resonator caused by material loading to the unloaded resonance frequency ω_r [8]:

$$\frac{\Delta\omega_r}{\omega_r} = -\frac{\iiint_{V_C}\left(\Delta\varepsilon\cdot|E_r|^2 + \Delta\mu\cdot|H_r|^2\right)dV}{\iiint_{V_C}\left(\varepsilon\cdot|E_r|^2 + \mu\cdot|H_r|^2\right)dV}. \quad (1)$$

In this application the volume integration is reduced to a line integration along the transmission line and the material under test will only change its dielectric constant. This simplifications reduces the classical formulation to:

$$\frac{\Delta\omega_r}{\omega_r} = -\frac{\int_{\text{line}}\Delta\varepsilon\cdot|E_r|^2 dx}{\int_{\text{line}}\left(\varepsilon\cdot|E_r|^2 + \mu\cdot|H_r|^2\right)dx}. \quad (2)$$

Using the similarity between wave equation and telegrapher's equation, E can be replaced by the voltage V, H by the current I and the material properties ε and μ can be expressed in terms of circuit elements. For the lumped element CRLH TL the integration is reduced to a summation over the n_C unit cells. The consideration of several resonance modes finally leads to a system of equations that relates the capacity changes to the changes in resonance frequencies:

$$\begin{pmatrix}\Delta\omega_{r,1}\\ \vdots \\ \Delta\omega_{r,n_C}\end{pmatrix} = \begin{pmatrix}a_{1,1} & \cdots & a_{1,n_C}\\ \vdots & & \vdots \\ a_{n_C,1} & \cdots & a_{n_C,n_C}\end{pmatrix}\begin{pmatrix}\Delta\varepsilon_1\\ \vdots \\ \Delta\varepsilon_{n_C}\end{pmatrix} \quad (3)$$

where the vector $\mathbf{\Delta\varepsilon}$ represents the changes in the dielectric constants of the liquid in the channels and the vector $\mathbf{\Delta\omega_r}$ corresponds to the resonance frequency shifts. Both vectors consist of n_C elements and, hence the dimension of the matrix $\mathbf{A}$ is $n_C \times n_C$. This derivation is described in detail in [9]. The capacity profile $\mathbf{\Delta\varepsilon}$ can be straightforward calculated from the relative resonance frequency shifts $\mathbf{\Delta\omega_r}$ using the inverse of $\mathbf{A}$

$$\mathbf{\Delta\varepsilon} = \mathbf{A}^{-1}\cdot\mathbf{\Delta\omega_r}. \quad (4)$$

Fundamental for a good sensor performance is the precise knowledge of $\mathbf{A}$. Experimentally it can be determined by successive measurements of the frequency shifts $\mathbf{\Delta\omega_n}$ when specific dielectric test patterns are applied to the structure. Details of this procedure are explained in [9]

III. Design

The design of a sensor is divided into two phases: First, the determination of equivalent circuit parameters and second the transfer of the equivalent circuit into a real layout. Initially the parameters of the equivalent circuit according to Fig. 1 have to be calculated based on the sensor specifications such as: center operation frequency, bandwidth, required sensitivity for the monitoring of a change in the dielectric constant of the liquids $(\Delta\varepsilon/\varepsilon)_{\min}$, number of required measurement channels, dynamic range of the S-parameter measurement system and frequency resolution for the detection of a shift in resonance frequency $(\Delta\omega_r/\omega_r)_{\min}$. Additionally it turns out that the sensor should be operated in the left-handed band of the CRLH TL because it is beneficial in terms of bandwidth requirements [7]. With these parameters a set of equations can be formulated describing the system performance. Due to limited space we cannot describe the full details in this paper and refer to [7] and [9]. Since it is not a linear system we use an iterative process to find solutions for the parameters C_L, L_L, C_R, L_R and the ratio between the fixed and the variable capacitance C_0 and C_M. Generally, there exist several solutions, but not all of them are realizable with a certain fabrication technology.

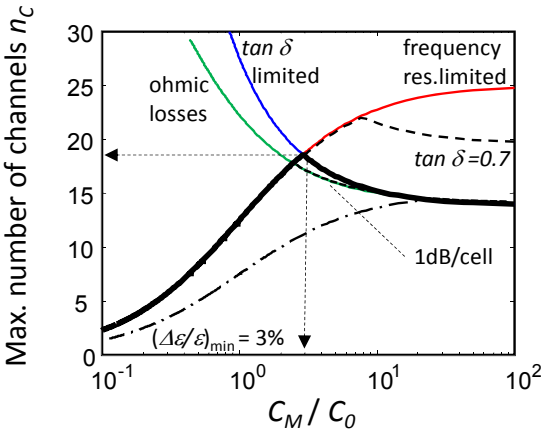

Figure 2. Calculated maximal number of measurement cells n_C versus ratio between C_M and C_0. Unless otherwise noted the curves are based on the following set of parameters: sensitivity for the detection of changes in the monitored dielectric constant $(\Delta\varepsilon/\varepsilon_r)_{\min}$ = 5%; losses of the liquid under test: $tan\ \delta$ = 1; dynamic range of the measurement system: 60 dB; accuracy for the detection of shifts in resonance frequencies $(\Delta\omega_r/\omega_r)_{\min} = 10^{-3}$; losses in the lumped element capacitors and inductors are neglected.

The ratio C_M/C_0 has to been chosen with respect to the requirements on sensing accuracy $(\Delta\varepsilon/\varepsilon_r)_{\min}$, system parameters and especially the losses of the liquid under test. For clarification purpose Fig. 2 shows in an example the influence of this ratio to the maximal number of measurement channels for a typical system configuration as listed in the figure caption. The maximal 18 cells are obtained for a ratio of C_M/C_0 = 3 as marked with arrows in the graph. For smaller values the frequency resolution for the detection of shifts in resonance peaks and for larger values the losses due to the liquid under test limit the number of channels n_C. This behavior is depicted in Fig. 2 with two labeled curves. The graph also shows exemplarily the influence of ohmic losses in the reactive line elements (1dB loss/cell), the change in the curve if the liquid has lower loss ($tan\ \delta$ = 0.7) and the influence of a change in $(\Delta\varepsilon/\varepsilon)_{\min}$ from 5% to 3%.

In the second step the most suitable solution has to been transferred into a layout, verified and optimized with full wave electromagnetic simulation. In our case we used CST Microwave Studio to simulate a sensor design using coplanar waveguides (CPW).

IV. Fabrication

Several different sensor layouts with one, two and four unit cells have been designed and fabricated. After cleaning the quartz substrates a photoresist is spin-coated and patterned using UV photolithography. The wafer is then placed into an evaporating system, which enables the deposition of a seed layer of titanium followed by 0.3 µm thick gold layer. The metal is released during the elimination of the photoresist in a solvent bath of acetone. The fluidic part which is realized in polydimethylsiloxane (PDMS) may be prepared in parallel. The elaboration of the fluidic channels is performed through the replication of the elastomer in a silicon mould. This one is previously prepared with the pattern of a photoresist, which is used as a mask during the etching of a silicon substrate with a Reactive Ion Etching step. The depth of etching corresponds to the desired height of the channels. After the elimination of the photoresist mask and a surface treatment used to favor the peeling-off of the elastomer, the PDMS is poured on the silicon substrate and solidified with a curing step. The PDMS is then peeled off and assembled on the circuit metallization.

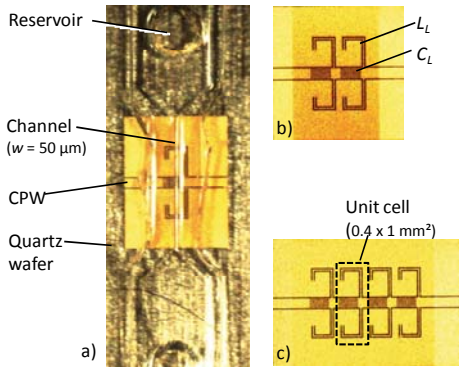

Figure 3. Photographs of some of the realized sensors. a) One unit cell with mounted microfluidic channel, b) two unit cells and c) four unit cells.

Fig. 3 shows the photograph of a realized sensor family. Additionally visible in Fig. 3a are the two microfluidic reservoirs used for filling of the channel and the channel itself with a width of 50 µm. The realization of the lumped element inductor L_L and capacitor C_L with a CPW stub line and an interdigital capacitance is depicted in Fig. 3b. The size of one unit cell of this sensor is 0.4 × 1 mm². For the control of the value C_M/C_0 a 4 µm thick SiO_2 layer has been inserted between the metallization and the channels.

V. Measurement

To prove the concept measurements have been done by filling the channels with water and different concentrations of water and ethanol mixtures. To insert the liquid into the channel, a small droplet was placed on one of the holes in the PDMS over the reservoirs. By applying underpressure on the other hole the liquid flows through the channel. The idea for the one channel structures is to fill the channel successively with liquids with different dielectric constants and to monitor the frequency shift. As stated in (3) we expect a linear relation between the dielectric of the liquid and the relative change of resonance frequency $\Delta\omega_r/\omega_r$ if the change in the capacitance is less than 10% [7]. For these tests the following procedure has been employed:

0. Determination of the unloaded resonance frequency by an empty channel measurement.
1. Measurement of the largest frequency shift by using the liquid with the highest dielectric constant (water in this case).
2.-7. Measurement of interim values using liquids with lower dielectric constant

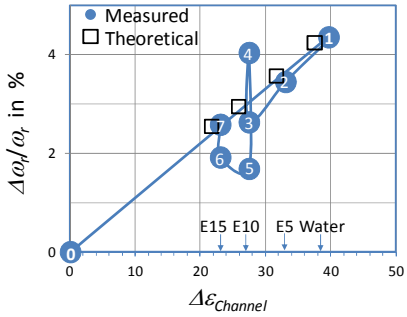

	Ethanol	Water
E5	5%	95%
E10	10%	90%
E15	15%	85%

Figure 4. Characterization of a one unit cell device with different liquids as depicted in Fig. 3a. In theory a linear dependence between the dielectric constant of the liquid under test and the shift in resonance frequency is expected.

Between the measurements 1-7 the channels were emptied and the unloaded resonance frequency was measured. Fig. 4 shows exemplary results of these tests. The sequence of the measurements is indicated with the numbers in the dots. Intermediate unloaded measurements with empty channels are not displayed. Blue dots show the actual measured values and the black squares represent the values expected from theoretical considerations. The graph reveals problems that were observed with a lot of structures. Following the measurement procedure described above for one liquid under test e.g. 10% ethanol and 90% water (e10), different values for the frequency shifts are obtained. The too low values can be explained with problems associated with filling of the 50 µm channels, the too high values are supposed to originate from bad adhesion of the channels. The liquid under test can penetrate into the structure between the PDMS film and the metallization. This assumption is confirmed by observations with the microscope during the filling of the channels.

Despite this technological problem we were able to make successful test measurements with some two channel structures but not with the four channel structures. Figure 5a shows the measured input reflection coefficient S_{11} of the structure from Fig. 3b from measurement and simulation. The main peak at 25 GHz is similar for both curves but there is a difference in the resonance around 19 GHz for the simulated and 17 GHz for the measured data. Additionally the measured losses in the structure are significantly higher above 20 GHz. This discrepancy is attributed to a deviation of the properties of the used materials like the evaporated gold and PDMS from their ideal behavior. However, since the elements of the matrix A are determined from calibration measurements this should have no influence on the performance of the sensor.

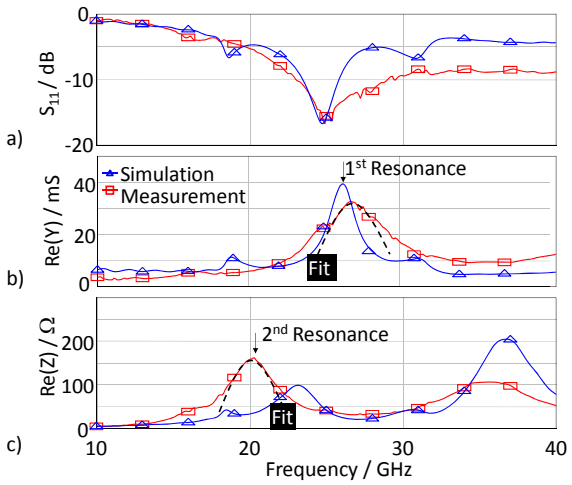

Figure 5. Example for a) the S-parameters and b) Y- and c) Z-parameters of a two cell sensor, where both channels are filled with water.

After the measurement the S-parameter data is transformed to Z- and Y- parameters. Fig. 5b and c show the plot of their real parts, which are used for the detection of resonances. In this case the resonator is analyzed as a one port open-ended device. Hence the first resonance can be detected with a maximum in the real part of the admittance Y, for the detection of the second resonance the Z-parameters are employed. Further resonances can be detected, if necessary, by the alternating analysis of Z- and Y-parameters. In order to increase the accuracy of detection the actual resonance frequencies are determined by a local curve fitting procedure around the maxima. The corresponding fitting curves are depicted with dashed lines in Fig. 5b and c.

Fig. 6 shows some examples for the monitoring of two microfluidic channels using the multi-resonant perturbation method. Different combinations and sensors have been tested. The observed accuracy is within what was expected and could clearly resolve the difference between pure water and water with 5% ethanol content (E05). The results were reproducible unless leakage of the channels was observed. Prior to the measurement the determination of the matrix A was done by applying specific filling patterns with water-filled and empty channels.

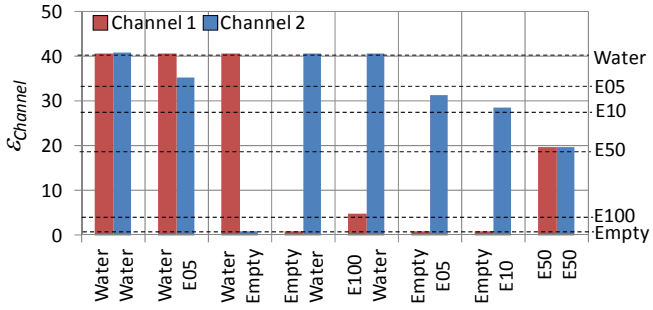

Figure 6. Examples for the monitoring of two microfluidic channels using the multi-resonant perturbation method. The lower part of the figure lists the liquids injected into the two channels, whereas the chart in the upper part shows the extracted values of the dielectric constant.

VI. Conclusion

The paper presents a concept for the simultaneous dielectric monitoring for substances like cells or chemicals in microfluidic channels at microwaves without any switching. The sensor consists basically of a CRLH TL which has been chosen to minimize the required bandwidth. One capacitor in each unit cell of the CRLH TL is electromagnetically coupled to a microfluidic channel, so that dielectric properties of the filling liquid influence the properties of the transmission line. For the extraction of the individual capacitance values the multi-resonant perturbation method is employed. The design and fabrication of prototype sensors is briefly described. Finally the measurements of the realized sensors are discussed.

The characterization of single channel structures revealed problems with the leakage of the channels, which is supposed to be the reason for the malfunctioning of the four channel sensors. However the sensor principle could be demonstrated with two channel sensors which allowed the monitoring of water / ethanol mixtures. Next steps will be the improvement of the technological process and a redesign of the structures towards a larger number of measurement channels.

Acknowledgment

We would like to acknowledge the support of the company CST - Computer Simulation Technology.

References

[1] A. Treizebré, et.al., “THz microscopic investigation on living cells”, *5th International Conference on Microtechnologies in Medicine and Biology*, April 1–3, 2009, Québec, Canada.

[2] K. Grenier, D. Dubuc, P.-E. Poleni, M. Kumemura, H. Toshiyoshi, T. Fujii, H. Fujita, H., "New broadband and contact less RF / microfluidic sensor dedicated to bioengineering," *Int. Microwave Symp 2009.*, pp.1329-1332, June 2009.

[3] C. Liu, Y. Pu, “ A microstrip resonator with slotted ground plane for complex permittivity measurements of liquids,” *Wireless Comp. Lett.*, Vol. 18, no 4, pp. 257-259, April 2008.

[4] S.Seo, T. Stintzing, I. Block, D. Pavlidis, M. Rieke, P.G. Layer, “High frequency wideband permittivity measurements of biological substances using coplanar waveguides and application to cell suspensions,” *Int. Microwave Symp, 2007.*, pp.915-918, June 2008.

[5] J. Mateu, N. Orloff, M. Rinehart, J.C. Booth, "Broadband Permittivity of Liquids Extracted from Transmission Line Measurements of Microfluidic Channels," *Int. Microwave Symp, 2007.*, pp.523-526, June 2007.

[6] K. Grenier, D. Dubuc, M. Poupot, J.-J. Fournié, "Microwave signatures of alive B-lymphoma cells suspensions," *Biomedical Wireless Technologies, Networks, and Sensing Systems (BioWireleSS),* vol., no., pp.95-98, Jan. 2011.

[7] M. Schüßler, M. Puentes, C. Mandel, R. Jakoby, "Multi-resonant perturbation method for capacitive sensing with composite right/left-handed transmission lines," *Int. Microwave Symp* , pp.481-484, 23-28 May 2010.

[8] L. F. Chen, C. K. Ong, C. P. Neo, V. V. Varadan, and V. K. Varadan, *Microwave Electronics*. Wiley, 2004.

[9] M. Schüßler, C. Mandel, M. Puentes, R. Jakoby, "Capacitive level monitoring of layered fillings in vessels using composite right/left-handed transmission lines," *Int. Microwave Symp 2011*, pp.1-4, 5-10 June 2011.